Advanced Seismic Magnitude Classification Through Convolutional and Reinforcement Learning Techniques

Qiuyi Lin, Jin Li*
School of Architectural Engineering, Chuzhou Polytechnic, Chuzhou 239000, Anhui, China

***Abstract*—Earthquake Early Warning (EEW) systems are crucial in reducing the dangers associated with earthquakes. This paper delves into the realm of EEWs, focusing on rapidly determining earthquake magnitudes (EMs). Traditional methods for swift magnitude categorization often grapple with challenges such as data disparity and cumbersome processes. Our research introduces an innovative EEW model, employing a 7-second seismic waveform record from three different components provided by the China Earthquake Network Center (CENC). This empirical, quantitative study pioneers a method combining dilated convolutional techniques with a novel mutual learning-based artificial bee colony (ML-ABC) algorithm and reinforcement learning (RL) for EM classification. The proposed model utilizes an ensemble of convolutional neural networks (CNNs) to simultaneously extract feature vectors from input images, which are then amalgamated for classification. To address the imbalances in the dataset, we implement an RL-based algorithm, conceptualizing the training process as a series of decisions with individual samples representing distinct states. Within this framework, the network operates as an agent, receiving rewards or penalties based on its precision in distinguishing between the minority and majority classes. A key innovation in our approach is the initial weight pre-training using the ML-ABC method. This technique dynamically optimizes the "food source" for candidates, integrating mutual learning elements related to the initial weights. Extensive experiments were carried out on the selected dataset to ascertain the most effective parameter values, including the reward function. The findings demonstrate the superiority of our proposed model over other evaluated methods, highlighting its potential as a robust tool for EM classification in seismology. This research provides valuable insights for both seismologists and developers of EEW systems, offering a novel, efficient approach to earthquake magnitude determination.**

Keywords*—Earthquake early warning; the magnitude of the earthquake; imbalanced classification; artificial bee colony; reinforcement learning

I. Introduction

The importance of earthquake prediction research is increasing globally, aiming to mitigate earthquake impacts. Early warning systems can drastically reduce casualties and damages from severe earthquakes [1]. These systems, endorsed by the United Nations, detect seismic activities and issue alerts rather than predicting earthquakes. Utilizing the time difference between primary and secondary seismic waves, they send warnings once an earthquake is detected. This allows immediate actions like unlocking building exits, managing power grids, and adjusting operations in critical facilities like hospitals and nuclear power plants [2].

The EEW system has gained significant attention in seismology research, particularly focusing on the "excellent period method" introduced by Nakamura et al. [3] and refined by Allen and Kanamori [4], which estimates earthquake magnitude from the initial three to four seconds of P-wave data. Despite its promise, this method shows notable variability in its estimates. To improve it, Kanamori [5] applied wavelet analysis for a more detailed time-frequency analysis of seismic data, but the problem of variability remained. Lancieri and Zollo [6] proposed an alternative, the "peak ground motion displacement Pd method," which uses peak displacements measured shortly after the P- and S-waves to estimate magnitude. Like its predecessors, this method also suffers from dispersion issues. Overall, current methods for magnitude estimation offer some level of estimation capability but are often limited by significant dispersion and lack of universal applicability.

Class imbalance, where one category has more data than the other, can adversely affect the performance of classification models [7]. The challenge is greater with minority classes due to their smaller size and variability. To address this, two main strategies are employed: data-level and algorithmic-level adjustments. At the data level, one can balance classes by over-sampling the minority class or under-sampling the majority class, but these methods risk information loss and overfitting [7, 8]. While these techniques are promising, their success varies depending on the dataset and application at hand, making it crucial to consider the specific characteristics of the imbalance and the needs of the application when choosing a method [9, 10]. Deep Reinforcement Learning (DRL) [11] has shown promise in improving classification by reducing noise and enhancing features, despite increasing computation time due to complex agent-environment interactions [12, 13]. DRL has been used to improve classifiers and in ensemble pruning, yet its application in addressing class imbalance has not been sufficiently explored by researchers [14].

Deep learning models have revolutionized multiple fields with their ability to fine-tune internal parameters through learning algorithms, particularly using backpropagation [15-18]. This method adjusts the weights of the model to minimize errors, but it can suffer from problems like sensitivity to initial weight settings and getting stuck in local minima, particularly

in classification tasks [19]. To overcome these issues, researchers are looking into meta-heuristic algorithms such as the ABC algorithm [20], which searches the solution space more broadly and is thus less likely to fall into local minima. However, the ABC algorithm itself has challenges in choosing the optimal food source or solution [21]. A new approach, ML-ABC, has been developed to enhance the standard ABC [22]. This method promotes mutual learning between different elements of the algorithm, improving adaptability and possibly resolving the weight initialization issues that affect gradient-based methods [23]. By fostering information exchange within the optimization process, ML-ABC can avoid local minima and find better solutions [24].

This research presents a deep learning model designed for EEW systems, which can accurately detect seismic events with magnitudes of 4 or higher using data from the first 7 seconds after the P-wave arrival from a single seismic station. The model uses dilated convolutional layers for feature extraction, which are then used for classification into two categories: EM ≥4 or EM <4. The data is skewed, with the EM ≥4 category being overrepresented, which adversely affects the model's performance. To tackle the data imbalance, the study applies a RL approach, where an agent iteratively learns from the environment to make binary classifications, receiving rewards for correct predictions and penalties for mistakes. A higher reward is given for correctly predicting the underrepresented class to address the imbalance. The agent aims to maximize classification accuracy and cumulative reward. The paper also addresses the issues of gradient-based training methods, which are sensitive to initial weight settings. The innovative ML-ABC method is introduced as a solution. It dynamically adjusts the optimization process by mutual learning from the initial weights, which improves the model's robustness. The model demonstrates outstanding performance in EEW tasks, with classification accuracy exceeding 90%. The paper highlights the effectiveness of combining DL with RL and the novel ML-ABC method for addressing data imbalance and initialization sensitivity in classification tasks. Below is a succinct summary of the primary themes explored within this paper:

- The article addresses the issue of imbalanced classification by introducing a sequential decision-making RL algorithm.
- Rather than relying on random weight assignments for model parameters, an enhanced ABC algorithm is adopted to establish initial values and a coding strategy for these parameters.
- A unique reward mechanism is integrated into the approach, incentivizing accurate decisions while penalizing errors. This mechanism assigns higher rewards to the minority class, prompting the model to allocate adequate attention to less common data. This strategic adjustment fosters a more equitable and balanced classification process.

The subsequent sections of the paper are organized as follows: Section II presents related works, while Section III provides an in-depth exploration of the proposed approach, detailing the core methodology. Section IV presents the empirical results and their subsequent analysis. In Section V, concluding remarks are provided, along with potential directions for future research.

II. Related Work

As the pool of seismic activity data grows, deep learning is becoming a cornerstone in the development of EEW systems. Ren et al. [25] capitalized on this by implementing CNNs to estimate earthquake magnitudes, treating the process as a classification problem. Their innovative model analyzes 4-second waveform segments from individual seismic channels to determine the potential impact of an earthquake. This approach has been validated through its successful application to distinct earthquake events, such as the clusters in Changning and Tangshan, proving its effectiveness in practical scenarios. Beyond academic validation, the model has seen real-world application, having been adopted by the China Earthquake Network Center (CENC) for real-time seismic data analysis, thus contributing to more timely and reliable earthquake warnings. Wang et al. [26] proposed a sophisticated deep learning model using long short-term memory (LSTM) neural networks to enhance onsite EEW systems. By analyzing the initial P waves to predict destructive S waves, this approach aims to mitigate the limitations of fixed-threshold single indicators, addressing complex nonlinearities due to varying travel paths and site effects. The LSTM model's proficiency was validated by testing it with recent seismic events in Taiwan, achieving remarkable accuracy with a 0% missed alarm rate and a mere 2.01% false alarm rate.

Expanding the scope of DL in EEW, Hu and Zhang [27] have designed a DL model that predicts the range of earthquake magnitudes with greater precision and reliability than traditional models. Despite its sophistication, this model could be prone to overfitting when faced with limited or noisy data, which might limit its application to new seismic events. Wang et al. [28] have pushed the boundaries further with DLcav, a CNN model aimed at predicting the cumulative absolute velocity (CAV) from seismic waveforms. DLcav stands out for enhancing the prediction of earthquake-induced damage, which is a crucial component of EEW. Datta et al. [29] introduced DeepShake, a novel deep spatiotemporal recurrent neural network designed for forecasting shaking intensities using real-time ground-motion data. This network-based model predicts future shaking across an array of stations without prior knowledge of their locations, learning from data on wave propagation patterns. Tested in the 2019 Ridgecrest earthquake sequence, DeepShake successfully alerted for significant shaking events with an equal error rate of 11.4%, indicating its potential as a reliable one-step early warning system for earthquakes.

Kavitha et al. [30] advanced the field of EEW through their development of the 3S-AE-CNN model, a novel innovation in deep learning applications. This model excels in quickly assessing crucial earthquake parameters, such as size and location, immediately after detecting the initial P-wave. The integration capabilities of this model with Internet of Things (IoT) technology could revolutionize the responsiveness of EEW systems. In a similar vein, Yanwei et

al. [31] have presented EEWNet, a cutting-edge deep learning framework that promises to rapidly and accurately predict earthquake magnitudes by analyzing raw P-wave data from single seismic stations. This model is particularly adept at dealing with earthquakes in the magnitude range of 4.0 to 5.9, offering a considerable improvement over existing empirical method.

Meanwhile, Meng et al. [32] have introduced an EEW model that leverages a DenseBlock structure with a Bottleneck and Multi-Head Attention mechanism to classify earthquake magnitudes from 7-second seismic data snippets. However, the model performance could be compromised by the issue of imbalanced data, which poses a risk to its predictive capabilities, especially for less frequent but critical earthquake magnitudes. Lastly, Lin et al. [33] have developed a CNN tailored for magnitude prediction, utilizing just 3-second windows of seismic data and conceptualizing the task as a classification problem, reinforcing the trend towards integrating advanced DL techniques in EEW for enhanced magnitude estimation accuracy. Münchmeyer et al. [34] proposed TEAM-LM, a hybrid model integrating CNN and Transformer architectures for simultaneous magnitude and location prediction using 10 seconds of data. While demonstrating promise within EEW systems, its computational intensity and multi-parameter predictions could impact overall accuracy.

III. Materials and Methods

The structure of the proposed model is shown in Fig. 1. The proposed model is particularly designed to enhance the classification process in seismic data analysis, where the intricacies of imbalanced classes and the necessity for precise initial weight settings are crucial. The adoption of ML-ABC and RL within our model directly addresses these critical areas where existing models fall short. Traditional algorithms often fail to offer a systematic method for initial weight selection, which can hinder the learning phase by causing slower convergence and the risk of settling on suboptimal minima. This can be particularly problematic in seismology, where the timeliness and accuracy of predictions are paramount.

Moreover, current models are not adequately equipped to deal with class imbalance, a frequent issue in seismic data where large magnitude events are rare. These models tend to be biased towards the majority class, resulting in a significant oversight of minority classes which are often the most critical to detect accurately in the context of earthquake early warning systems. Our approach, through ML-ABC, provides a carefully considered and diverse set of initial weights, enhancing the model's ability to escape local minima and converge more efficiently to a global solution.

Furthermore, the RL component of our model is tailored to assign a higher reward to the correct classification of the minority class, effectively shifting the model's focus towards these critical predictions. This is a substantial improvement over traditional supervised learning methods, which may not have sufficient representative data to train effectively across all classes. RL's adaptability in the learning policy allows for a more balanced exploration of the decision space, leading to strategies that favor the accurate classification of underrepresented classes. This adaptive nature of RL in our model sets it apart from existing methods, equipping it to overcome the inherent limitations faced by conventional classification approaches in the context of EEW systems.

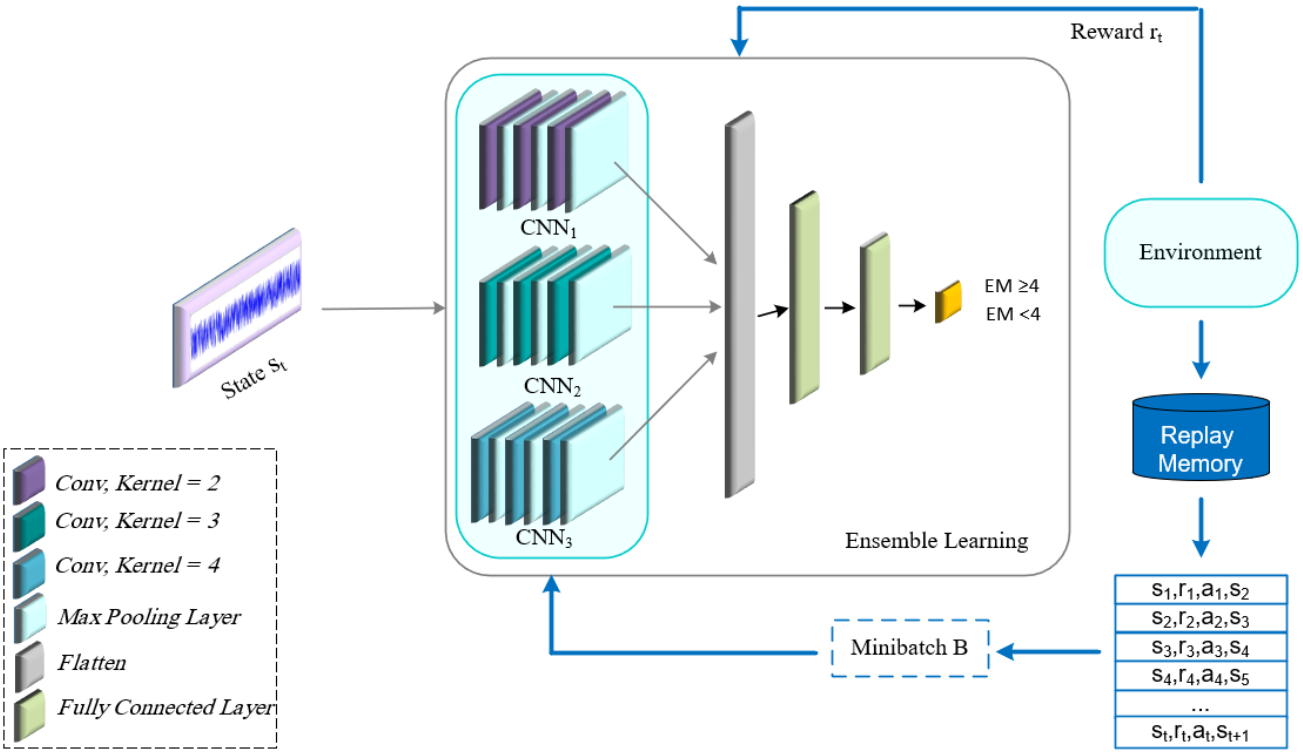

Fig. 1. The proposed model.

A. Pre-training Phase

The accuracy of network weights' initial values holds significant importance for deep models. If these initial settings are inaccurate, their repercussions can cascade throughout the model's training process, potentially leading to challenges related to convergence. Acknowledging the pivotal role of weight initialization, the initial phase of this study embarks on establishing the optimal configurations for both the CNN and the feed-forward neural network. To address the predicament of weight initialization, we introduce a groundbreaking approach called the ML-ABC technique. This strategy seeks to revolutionize the conventional process of determining initial values for network weights. In typical scenarios, the selection of initial weights relies on various methods, often incorporating heuristic or random techniques. However, the ML-ABC method introduces a higher level of intelligence into this process. By combining the principles of artificial bee colony optimization with the concept of mutual learning, the ML-ABC approach draws inspiration from the cooperative behaviors observed in natural bee colonies. This innovative approach aims to generate optimal initial weight seeds by enabling the network to learn and evolve collaboratively through the exchange of insights and knowledge. This facilitates a more informed and efficient weight initialization process.

1) The ML-ABC algorithm: The ABC algorithm, drawing inspiration from the intricate behaviors of honeybees when foraging for food, mirrors the collective intelligence and intricate actions observed in nature. This algorithm provides a methodical and intuitive approach to solving optimization problems. At its core, the ABC algorithm comprises four essential components:

a) Worker Bees: Functioning as the initial explorers, these bees venture into a designated area or target zone to identify potential food sources. Their actions are not random but are guided by their knowledge of previous sources, evaluating the quantity and quality of nectar available. After gathering information, they return to the hive to share their findings.

b) Observer Bees: Situated within the hive, observer bees absorb and analyze the information brought by the worker bees. Their decisions are based on shared information, particularly the quality and quantity of nectar discovered. If a worker bee's dance (used to communicate food source information) is compelling and suggests a rich source, observer bees are influenced to visit that location. This dance-based decision-making process ensures the swift exploitation of promising food sources.

c) Scout Bees: These bees act as adventurers, stepping in when a food source becomes depleted or no longer viable. Rather than relying on dance-based information, scouts explore the surroundings to find fresh food sources in a stochastic manner. Their role ensures the hive's adaptability and resilience to changing conditions.

d) Food Sources: Representing potential solutions to the optimization problem, each food source possesses a nectar quantity that reflects the quality or fitness of the associated solution. The collective aim of the worker bees, observer bees, and scouts is to maximize nectar accumulation, analogous to seeking optimal solutions in a computational context.

The brilliance of the ABC algorithm lies in its adaptability. By mimicking the foraging behaviors of honeybees, it achieves a balance between exploring new solutions and exploiting known ones. This intricate interplay of roles and responsibilities, guided by nature-inspired principles, positions the ABC algorithm as a robust tool in the realm of optimization [35].

Eq. (1) elucidates the process of generating a new position, utilizing spatial information from the worker bee. If the nectar found at the new position surpasses the quality of the previous location, the bee will adopt the new position, abandoning the former one. Conversely, if the quality of the nectar is subpar, the bee retains the memory of its previous location.

$$v_i^j = s_i^j + \varphi_i^j (x_i^j - x_k^j) \tag{1}$$

The equation employs the index i to represent the i-th position, where each solution s_i comprises a set of D parameters. The parameter D signifies the count of parameters subjected to optimization, while k signifies an alternative random solution distinct from i. The variable φ_i^j is randomly chosen from the interval [0, 1]. Introducing a change to one parameter of s_i generates a novel solution v_i, which may differ from the original one.

During an optimization process in "D" dimensions, a dimension is randomly selected, and its value is adjusted, with the fitness value determining the superior outcome in each iteration. As indicated in Eq. (1), the novelty and irregularity of the fresh food source v_i^j stem from its dependence on two variables, s_i^j and s_k^j.

To create a food source with enhanced fitness, we leverage knowledge derived from mutual learning between the present and adjacent food sources. This aspect is pivotal in the ABC algorithm, as it necessitates a food source with a heightened fitness value [36].

$$v_i^j = \begin{cases} s_i^j + \varphi_i^j (s_k^j - s_i^j), & Fit_i < Fit_k \\ s_k^j + \varphi_i^j (s_i^j - s_k^j), & Fit_i \geq Fit_k \end{cases} \tag{2}$$

where, Fit_i and Fit_k denote the fitness values of the neighboring and current food sources, respectively. The variable φ_i^j is a uniformly distributed random integer ranging from 0 to F, where F represents a positive mutual learning factor. Novel solutions enhance their fitness by evaluating nearby and current food sources and gravitating toward superior choices. If the current food source offers better fitness, the candidate solution aligns with it; otherwise, the solution moves toward a neighboring source. The stability of food positions hinges on the value of F, which must be a non-negative positive number yielding improved solution.

As the value of F incrementally rises from zero to a specific threshold, the disturbances observed in the corresponding point diminish. This signifies that the fitness value of the alternative food source is converging to, or

closely approaching, the higher fitness value. However, an elevated F value disrupts the delicate balance between exploration and exploitation. In order to illuminate the potential solution in the ML-ABC algorithm, our research's encoding technique vectorizes the CNN and feed-forward weights. It is challenging to provide precise weights, but through several attempts, we devised a method of encoding that strives for the utmost accuracy. An example of encoding a feed-forward network with three hidden layers and a CNN network with three layers, each layer comprising three filters, is shown in Fig. 2. The array's weight matrices are all referenced as rows, and this is crucial information to remember.

For the purpose of determining how effectively a solution fits into the developed DE algorithm, the fitness factor is constructed as follows:

$$Fitness = \frac{1}{1+\sum_{i=0}^{N}(y_i-\tilde{y}_i)^2} \quad (3)$$

The y_i and $\tilde{y}_i$ represent the target and projected labels, respectively, for the i-th dataset, while *N* indicates the total number of cases.

B. Deep Reinforcement Learning

DRL presents a robust approach within the realm of deep learning, where an agent dynamically engages with its environment to optimize rewards. This dynamic learning process equips the agent to navigate uncertain situations and make a sequence of decisions, proving particularly valuable in diverse domains like robotics, healthcare, and finance [37]. DRL's competence in handling tasks necessitating sequential decisions and its adaptability to unpredictable scenarios underscore its versatile, practical applicability. A primary challenge in tasks involving categorization arises from imbalanced datasets, where one category significantly outweighs others. This imbalance can lead to biased learning, as conventional categorization methods tend to prioritize the dominant category heavily, consequently hindering the recognition of less prominent ones. In such cases, DRL emerges as a more efficacious strategy for training neural networks compared to conventional methods. DRL tackles the uneven categorization issue by incorporating a reward-based system. By judiciously assigning rewards, the agent's attention can be steered towards instances from less prevalent categories, thereby enhancing the accurate identification of these infrequent groups. This incentive-driven model establishes a comprehensive decision-making approach, giving prominence to the detection and categorization of rare incidents or less common categories.

In the domain of deep Q-learning, the agent's objective is centered on selecting actions that maximize the potential rewards in forthcoming situations. The rewards expected in future scenarios, denoted by the reward value, decrease over time with the discount rate γ, as depicted in Eq. (3). In this context, T represents the final time step of an episode.

$$R_t = \sum_{t'=t}^{T} \gamma^{t'-t} r_{t'} \quad (4)$$

Q-values stand for the measure of state-action interactions' effectiveness and symbolize the predicted result of policy π when action a is taken in state s. This calculation is illustrated in Eq. (4).

$$Q^{\pi}(s,a) = E[R_t|s_t = s, a_t = a, \pi] \quad (5)$$

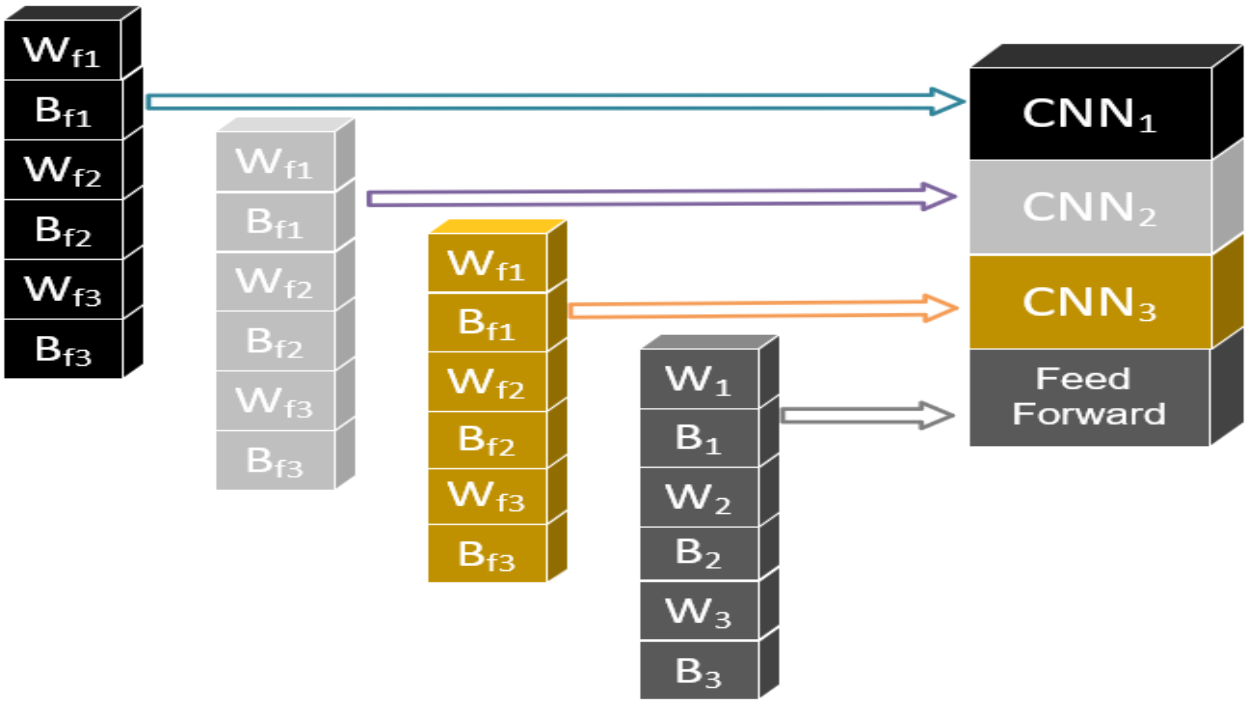

Fig. 2. Strategy for encoding employed in the algorithm being suggested.

The action-value function that yields the maximum expected reward among all strategies following the observation of state s and the execution of action a is computed as illustrated in Eq. (5).

$$Q^*(s,a) = max_\pi\, E[R_t|s_t = s, a_t = a, \pi] \quad (6)$$

The function applies the Bellman equation [38], which asserts that the highest expected result for a specific action is the combination of the current action's rewards and the maximum expected outcome from subsequent actions in the following step. This idea is illustrated in Eq. (6).

$$Q^*(s,a) = E[r + \gamma\, max_{a'} Q^*(s',a')|s_t = s, a_t = a] \quad (7)$$

The calculation of the optimal action-value function is conducted in a step-by-step manner utilizing the Bellman equation, as demonstrated in Eq. (7).

$$Q_{i+1}(s,a) = E[r + \gamma\, max_{a'} Q_i(s',a')|s_t = s, a_t = a] \quad (8)$$

During the training process, as the network encounters state s, it generates a corresponding action for that state. Subsequently, the environment provides a reward r and transitions to the next state s'. These variables are combined into a tuple (s, a, r, s'), which is then stored in memory M. Collections of these tuples, referred to as Batches B, are selected to perform gradient descent. The formula to compute the loss is described as shown in Eq. (8).

$$L_i(\theta_i) = \sum_{(s,a,r,s') \in B} (y - Q(s,a;\theta_i))^2 \quad (9)$$

In this context, θ represents the weights of the model, while y represents the estimated target for the Q function. This estimation involves summing the reward associated with the state-action combination and the discounted highest Q value in subsequent time steps, as demonstrated in Equation 9.

$$y = r + \gamma\, max_{a'} Q(s', a';\ \theta_{k-1}) \quad (10)$$

It is worth highlighting that the Q value assigned to the terminal state is set to 0. The magnitude of the gradient for the loss function at iteration i can be computed using Eq. (10).

$$\nabla_{\theta_i} L(\theta_i) = -2 \sum_{(s,a,r,s') \in B} (y - Q(s,a;\theta_i)) \nabla_{\theta_i} Q(s,a;\theta_i) \quad (11)$$

Through executing a gradient descent iteration on the loss function, the model's weights are updated as per Eq. (11). This adjustment aims to reduce the disparity, with α representing the learning rate that governs the degree of progress in the optimization process.

$$\theta_{i+1} = \theta_i + \alpha \nabla_{\theta_i} Q(s,a;\theta_i) \quad (12)$$

In this paper, our emphasis lies in applying the RL-driven algorithm in the realm of EEW. The following explanation elucidates the functioning of the methodology and imparts comprehension of each constituent element:

- State $\boldsymbol{s_t}$: This corresponds to the image observed at the time step t.
- Action $\boldsymbol{a_t}$: The classification performed on the image is treated as an action. This represents a decision made by the network based on its existing understanding of the goal.
- Reward $\boldsymbol{r_t}$: A reward is provided for each classification, designed to guide the network toward precise categorization. The formulation of this reward mechanism is presented as follows:

$$r_t(s_t, a_t, y_t) = \begin{cases} +1\,, a_t = y_t \text{ and } s_t \in D_O \\ -1\,, a_t \neq y_t \text{ and } s_t \in D_O \\ \lambda\,, a_t = y_t \text{ and } s_t \in D_N \\ -\lambda\,, a_t \neq y_t \text{ and } s_t \in D_N \end{cases} \quad (13)$$

Here, D_O and D_N respectively refer to the majority and minority classes. Accurately/incorrectly categorizing a sample from the majority class results in a gain/loss of $+\lambda/-\lambda$. The proposed method directs the network towards prioritizing the precise classification of instances from the rarer class, assigning a higher absolute value as a reward. Simultaneously, incorporating the majority class and a versatile reward parameter within the interval of $0 < \lambda < 1$ introduces intricacy to the reward structure, enabling precise tuning of the network's emphasis between the more prevalent and less common classes.

IV. Empirical Evaluation

A. Dataset

The data utilized in this investigation consists of three-component waveform data sampled at a frequency of 100 Hz. These data were collected by CENC from 1104 stations located in China over the time span from 2009 to 2017 [32]. As seismic waves propagate, their energy weakens as the distance of propagation increases. Consequently, the characteristics of waveforms tend to deteriorate. To address this, we have chosen seismic waveforms with epicentral distances shorter than 200 km. These waveforms might display disruptions and overlaps due to issues like network communication anomalies and equipment malfunctions. Therefore, we employ the "obspy" library to reprocess the data in this study. The composition of the training and test sets is presented in Table I.

TABLE I. Waveform Distributions for the Unbalanced Dataset Presented by CENC

Magnitude range	Waveforms in the CENC dataset
1-2	214963
2-3	91206
3-4	14080
≥4	4017

B. Metrics

We employ various metrics such as Accuracy, F-measure, and G-means, which are defined as follows:

$$\text{Accuracy} = \frac{TP+TN}{Total\ number\ of\ samples} \quad (14)$$

$$\text{Precision} = \frac{TP}{TP+FP} \quad (15)$$

$$\text{Recall} = \frac{TP}{TP+FN} \quad (16)$$

$$Specificity = \frac{TN}{TN+FP} \quad (17)$$

$$\text{G} - \text{means} = \sqrt{\text{Recall} \times Specificity} \quad (18)$$

Here, TP represents the true positives, or the count of actual positives accurately identified by the model. TN denotes the true negatives, referring to the actual negatives that the model correctly predicts. FP stands for false positives, which are the actual negatives that the model erroneously labels as positive. Lastly, FN indicates the false negatives, meaning the actual positives that the model incorrectly classifies as negative.

C. Comparator Models

During the evaluation phase, a comprehensive comparative analysis was conducted to assess the performance of our proposed model in comparison to five distinct deep learning frameworks: SeisNet [25], EEWMagNet [32], MagEstNet [39], QuakeClassNet [40], QuakeNet [41]. This rigorous examination aimed to offer a holistic perspective on our model's efficacy in relation to contemporary methodologies. To further explore various adaptations of our proposed model, two modified versions were introduced into the analysis. The first variant, referred to as "Proposed with RL," maintained an architectural design akin to our original model while excluding the application of the ML-ABC technique. Conversely, the second variant, "Proposed with ML-ABC," omitted the use of the RL technique for classification. To thoroughly evaluate the performance of these models, established metrics were employed, with a specific focus on metrics like the F-measure and geometric mean, known for their suitability in cases of skewed data distributions.

D. Results

The outcomes of this evaluation, as detailed in Table II, distinctly showcase the superior performance of our proposed model when compared to all other contenders, even including well-established models such as EEWMagNet and SeisNet. Across all evaluation criteria, our model consistently demonstrated its superiority over its counterparts. Remarkably, the model achieved substantial reductions in errors, showcasing improvements of 25% and 10% in the F-measure and G-means metrics, respectively. These noteworthy enhancements underscore the model's ability to effectively address challenges posed by imbalanced data distributions and its proficiency in delivering more accurate predictions.

A particularly illuminating comparison emerges when we consider the model's modified versions - "Proposed with RL" and "Proposed with ML-ABC". The advantages inherent in the integration of ML-ABC with the RL approach become evident. Our primary model achieved a substantial reduction in errors, nearly 30%, relative to its modified versions. This emphasizes the pivotal roles of both ML-ABC and RL in augmenting the model's performance, underscoring their significance in advancing the development of cutting-edge deep learning systems.

TABLE II. PERFORMANCE METRICS OF THE PROPOSED MODEL VERSUS COMPARATOR DEEP MODELS

	Accuracy	**F-measure**	**G-means**
EEWMagNet	0.8914±0.1405	0.8622±0.2001	0.8515±0.0104
SeisNet	0.8510±0.1553	0.7471±0.1054	0.8002±0.0402
MagEstNet	0.8105±0.1404	0.7302±0.1404	0.8006±0.1201
QuakeClassNet	0.7901±0.1006	0.5502±0.0953	0.6505±0.2502
QuakeNet	0.6703±0.1205	0.6702±0.2103	0.7503±0.0051
Proposed with RL	0.8104 ± 0.0627	0.7918 ± 0.1623	0.8303 ± 0.2622
Proposed with ML-ABC	0.8615 ± 0.0243	0.8506 ± 0.0517	0.8609 ± 0.0921
Proposed	0.9217 ± 0.0384	0.8814 ± 0.0297	0.9066 ± 0.0423

Table III presents a comparative analysis of the performance metrics for various deep learning models, including the proposed model, across two classes: EM <4 and EM ≥4. In the EM <4 class, the proposed model exhibits a superior performance with an accuracy of 0.9012±0.0450, indicating its robustness in this category. This performance is notably higher than that of EEWMagNet and SeisNet, which have accuracies of 0.8714±0.1210 and 0.8616±0.1020, respectively. MagEstNet and QuakeClassNet show moderate performance, while QuakeNet trails with the lowest accuracy in this class. For the EM ≥4 class, the proposed model again leads with an impressive accuracy of 0.9415±0.0056, significantly outperforming all comparator models. EEWMagNet, with an accuracy of 0.9012±0.0255, follows as the second most accurate model. SeisNet and MagEstNet show relatively similar performances, while QuakeClassNet and QuakeNet lag behind, indicating potential challenges in accurately classifying instances in this higher EM category. The consistency in the leading performance of the proposed model across both classes underscores its effectiveness and

reliability in binary classification tasks within this context. This superiority is particularly notable in the EM ≥4 class, where the margin of its lead suggests a higher degree of precision and confidence in its predictive capabilities. These results highlight the potential of the proposed model as a robust tool for classification in the studied domain.

Fig. 3 depicts the receiver operating characteristic (ROC) curves for the techniques outlined in Table I. The primary metric employed for assessing the effectiveness of classifiers is the area under the curve (AUC). An AUC value of 1 signifies perfect differentiation, while a value of 0.5 indicates performance equivalent to random chance. Among the various models, SeismoNet stands out with an impressive AUC score of 0.81. This remarkable result showcases its exceptional ability to distinguish between positive and negative outcomes, providing further evidence of the method's robust predictive prowess.

In contrast, both EEWMagNet and SeisNet demonstrated average AUC scores of 0.69 and 0.51, respectively, falling short of the performance achieved by our proposed model. The remaining models, including QuakeNet, QuakeClassNet, and QuakeNet, yielded less favorable results, exhibiting AUC scores ranging from 0.48 to 0.51. Notably, the performance of the QuakeNet model was notably lower, achieving a meager AUC of 0.48, just slightly surpassing the threshold for random prediction. The ROC curves vividly illustrate the disparities in performance across the evaluated methods, with our proposed model showcasing superior performance in discriminating between different outcomes.

Fig. 4 illustrates the error progression observed in the proposed model over a span of 500 epochs. Commencing with an initial error measurement of 10, a consistent downward trajectory becomes evident as the epochs advance. This sustained decline in error validates the model's ability to adapt and enhance its predictive capabilities with the accumulation of training iterations.

It is noteworthy that the most significant reduction in error occurs during the earlier epochs, gradually tapering off as the epochs accumulate. This pattern suggests diminishing returns in terms of error reduction as training prolongs, particularly after approximately the 425th epoch. Around this point, the error stabilizes, maintaining a relatively constant value of approximately 4.2962 across subsequent epochs. This plateau implies that continuing training beyond this juncture might not yield substantial performance improvements, implying the likelihood of the model reaching convergence.

Furthermore, this stability could serve as an indicator of potential overfitting, especially if there is no subsequent improvement observed on external validation or testing datasets. This underscores the importance of monitoring the model's behavior and performance to strike the right balance between training duration and preventing overfitting.

TABLE III. PERFORMANCE METRICS OF THE PROPOSED MODEL VERSUS COMPARATOR DEEP MODELS BY CLASS

Model / Class	EEWMagNet	SeisNet	MagEstNet	QuakeClassNet	QuakeNet	Proposed
EM <4	0.8714±0.1210	0.8616±0.1020	0.7914±0.2356	0.8015±0.1148	0.7014±0.1263	0.9012 ± 0.0450
EM ≥4	0.9012±0.0255	0.8423±0.1026	0.8216±0.1462	0.7726±0.1065	0.6425±0.1105	0.9415± 0.0056

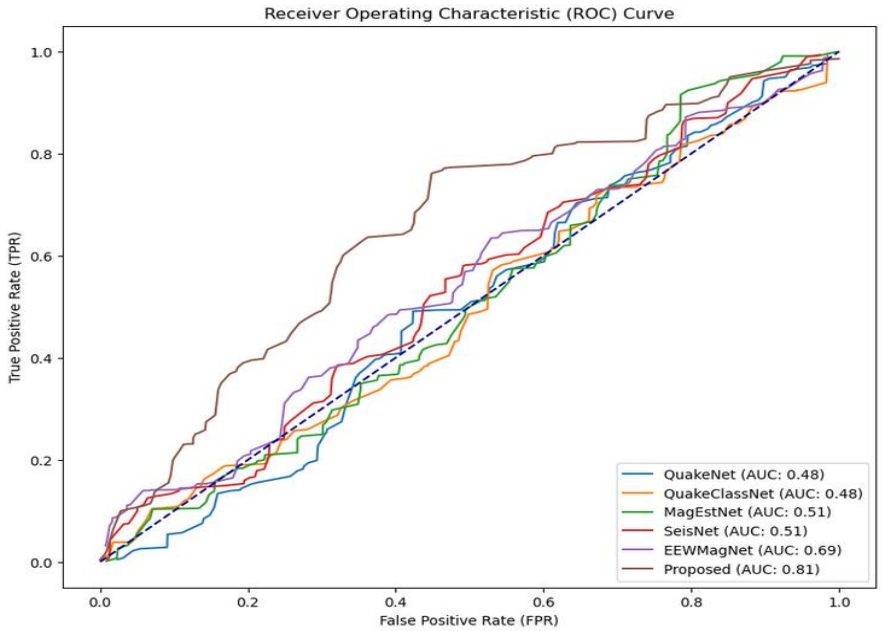

Fig. 3. The ROC chart illustrates the ROC curves for the proposed model and other benchmark techniques. The blue dashed line on the graph represents the ROC curve corresponding to random guessing.

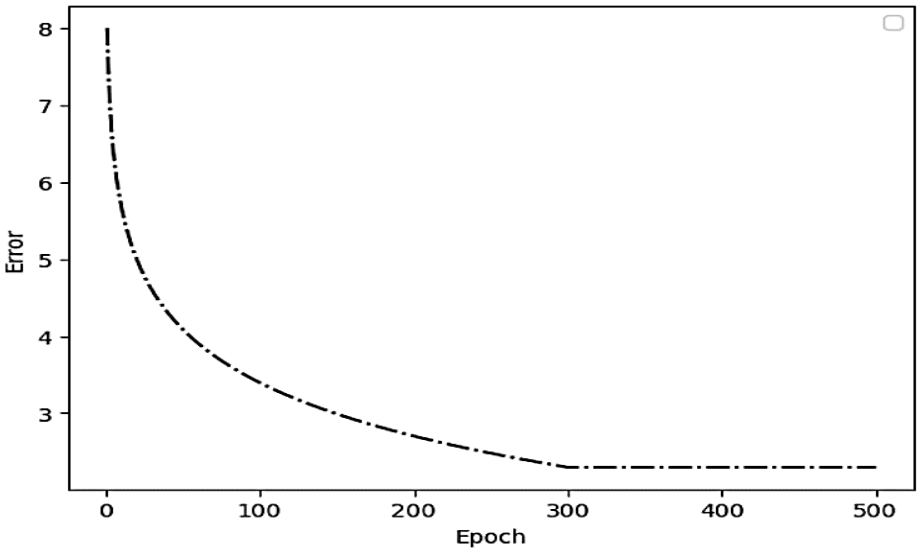

Fig. 4. Diagram illustrating the comparative dynamics of errors.

1) Impact of the reward function: Within our devised model, we introduced a reward mechanism to handle class imbalances effectively. In the case of the majority class, correct predictions were rewarded with a score of +1, while incorrect ones incurred a penalty of -1. For the minority class, accurate predictions garnered rewards of +λ, while incorrect ones resulted in penalties of -λ. The specific value of λ was adjusted based on the ratio between majority and minority samples. Notably, as this ratio increased, the optimal λ tended to decrease.

To explore the impact of λ, we thoroughly analyzed the model's performance across a spectrum of λ values ranging from 0 to 1, incrementing by intervals of 0.1. Throughout this analysis, the reward for the minority class remained consistent. The findings are presented in Fig. 5. At λ = 0, the influence of the majority class was minimal, while at λ = 1, both classes carried equal significance.

The data underscores that the model's most optimal performance is achieved when λ is set to 0.6, according to all evaluation criteria. This indicates that the most suitable value for λ resides between the extremes of 0 and 1. It is essential to recognize that while adjusting λ to diminish the dominance of the majority class is essential, setting it too low can potentially undermine the overall model performance.

This investigation highlights the critical role that the choice of λ plays in shaping the model's outcomes. Determining the ideal value of λ hinges on the relative frequency of majority and minority samples, emphasizing the significance of meticulous parameter adjustments to attain optimal result.

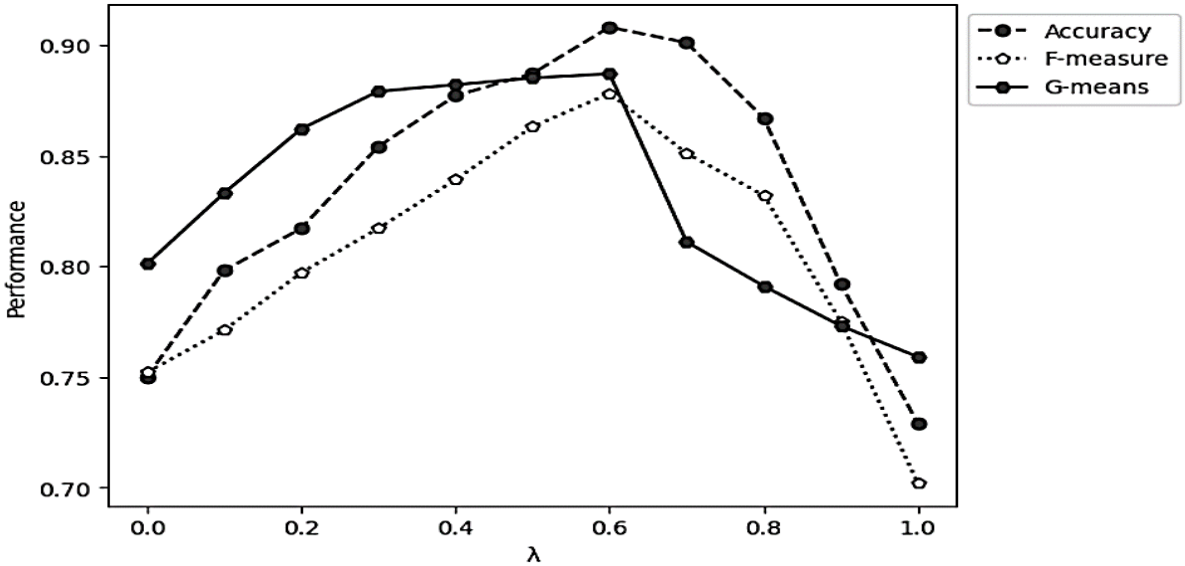

Fig. 5. Generating graphs illustrating the performance metrics of the proposed model as they vary in response to different λ values incorporated within the reward function.

2) Impact of the loss function: A wide array of strategies is available to tackle data imbalances within the realm of machine learning [42]. These encompass enhancements in data augmentation methodologies as well as the careful selection of an appropriate loss function. The pivotal role of the chosen loss function in enabling the model to capture the intricacies of the underrepresented class comprehensively cannot be overstated. Our investigation delved into the effectiveness of five distinct loss functions: Weighted cross-entropy (WCE) [43], balanced cross-entropy (BCE)] [44], Dice loss (DL) [45], Tversky loss (TL) [46], and Combo Loss (CL) [47].

While both WCE and BCE commonly utilized loss functions that treat positive and negative instances with equal weight, their performance may falter when faced with datasets exhibiting significant imbalances that heavily favor the minority class. On the contrary, DL and TL emerge as more suitable choices for datasets characterized by pronounced imbalances, showcasing notably improved results in relation to the minority class. Among these, CL takes a distinctive position as an exceedingly effective loss function, particularly tailored to datasets characterized by skewed distributions. Through judicious adjustments of the loss function's weights, CL elevates the significance of intricate samples, thereby conferring them a greater influence than straightforward ones.

Our meticulous analysis of these loss functions has been meticulously detailed in Table IV, yielding illuminating insights. The outcomes of this study underscore the exceptional performance of CL in comparison to TL, leading to an impressive 13% reduction in error rate accuracy and a substantial 25% enhancement in the F-measure, a pivotal metric for model evaluation. However, it is imperative to note that, despite its remarkable achievements, CL falls short by 20% when measured against our proposed model, which has been intricately designed to tackle binary classification challenges. This underscores the context-specific nature of model design and the need to tailor solutions to the particular problem at hand.

TABLE IV. COMPARISON OF THE PERFORMANCE METRICS BETWEEN THE SUGGESTED MODEL AND THE EMPLOYED LOSS FUNCTIONS

	Accuracy	F-measure	G-means
WCE	0.7432± 0.1132	0.7215± 0.0130	0.7510± 0.1255
BCE	0.8001± 0.1021	0.7622± 0.0102	0.8025± 0.0101
DL	0.8042± 0.2033	0.7992± 0.0106	0.826± 0.1000
TL	0.8320± 0.1203	0.8148± 0.0436	0.8450± 0.2062
CL	0.8630± 0.0247	0.8440± 0.0152	0.8639± 0.0152

3) Impact of the number of CNNs: The proposed architecture employs multiple CNNs to derive feature vectors from input images concurrently. The quantity of these CNN-based feature extractors significantly influences the model's performance. Utilizing an insufficient number of CNNs can lead to subpar feature extraction, while an excessive number might result in overfitting or the inclusion of redundant information. Both these extremes have the potential to undermine the efficacy of the model. To identify the ideal number of CNNs, an evaluation of the proposed model was conducted across a range of one to seven CNN feature extractors.

The outcomes of this investigation reveal that the model attains its peak performance when equipped with three CNNs, as clearly depicted in Fig. 6. Interestingly, the model's performance exhibited a decline when six and seven CNNs were employed. Strikingly, these cases even yielded results inferior to those obtained using a solitary CNN. This finding underscores the delicate balance required in selecting the number of CNNs for optimal performance, where an excess can prove detrimental rather than beneficial.

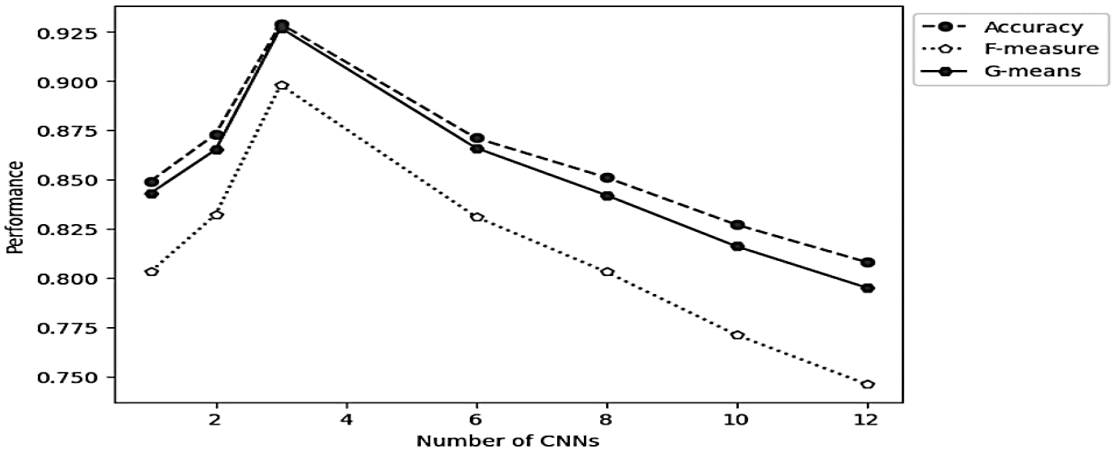

Fig. 6. Graphing the performance measurements of the suggested model concerning changes in the count of convolutional feature extractors.

4) Discussion: The study unveiled an innovative EEW model that was specifically designed to classify earthquake magnitudes rapidly. This classification was achieved through the analysis of a 7-second, three-component seismic waveform record acquired from the CENC. This novel model architecture featured a distinctive incorporation of three concurrent dilated convolution layers. These layers played a pivotal role in extracting crucial feature vectors that were subsequently employed for effective classification tasks.

Addressing the inherent challenges tied to data imbalances often encountered in conventional EEW models, the research integrated an algorithm based on RL. This strategic approach aimed to enhance the accuracy of sample classifications by providing appropriate rewards to the model. In the training process, individual samples were visualized as distinct states within a sequence of interconnected decision points. Functioning as an agent, the neural network received rewards or penalties based on its performance in accurately distinguishing between various classes.

To initiate the weight pre-training of the model, a unique approach known as ML-ABC was introduced. This pioneering technique dynamically adjusted the optimal "food source" for candidate solutions, encompassing components of mutual learning that were intricately linked to the starting weights. This innovative initialization process contributed to the ability of the model to learn and adapt during subsequent training phases.

The model proposal, crafted using seismic waveform records obtained from the CENC, exhibits potential limitations when attempting to extend its applicability to various global datasets. Its fundamental design, intricately linked to the distinct seismic characteristics unique to the CENC, raises substantial concerns regarding its performance when applied to regions such as California, renowned for the San Andreas Fault, or Japan, a significant participant in the Pacific Ring of Fire [48]. This potential challenge unfolds in two aspects: firstly, the model might internalize and overly emphasize the particular attributes of the CENC dataset, and secondly, it could inadvertently absorb any biases inherently present within that dataset. Such an excessively specialized adaptation could significantly hinder the capacity of the model to adapt to broader, more diverse contexts, impeding its generalization capabilities [32].

Furthermore, while the algorithms incorporated within the proposed model, such as RL and dilated convolution layers have been meticulously fine-tuned to accommodate CENC data, their flexibility when applied to unfamiliar datasets, remains questionable. A common issue observed with specialized algorithms is their susceptibility to overfitting on the training data, rendering them less adaptable and responsive when presented with previously unseen data. Take the RL algorithm, for instance, which has been structured with reward mechanisms tailored to the unique attributes of the CENC dataset [49]. This design might lead to challenges when confronted with datasets that possess distinct seismic event distributions. Similarly, the dilated convolution layers, optimized specifically to decipher intricate patterns inherent in CENC data, could either overlook or misinterpret vital features originating from divergent geographic regions [50].

The complexities inherent in seismic data are multifaceted, and the presence of noise or anomalies can wield substantial influence over the accuracy and dependability of any predictive model [51]. In regions marked by dense urbanization or significant industrial undertakings, the vibrations stemming from everyday human activities like traffic movement, construction endeavors, or even the operations of underground subway systems can introduce supplementary signals into the seismic data. Likewise, natural geophysical disturbances such as volcanic eruptions, landslides, or even robust winds and oceanic waves can engender disturbances that might be misconstrued as seismic activity by a model that hasn't been primed to contend with such factors [52].

The susceptibility of the proposed model to such extraneous signals takes on heightened concern when pondering the repercussions of erroneous alerts or missed predictions. The occurrence of false alarms, where the model inaccurately forecasts a seismic event due to noise, holds the potential to induce unwarranted panic and economic disruptions and erode public trust in the reliability of the system. Conversely, if the model fails to identify a genuine seismic event owing to its confusion with noise, the ramifications could be gravely severe, encompassing loss of lives and property.

Furthermore, managing noise isn't merely a matter of filtering out undesired signals; it also necessitates the ability to discriminate between noise and legitimate seismic activities that might exhibit similar characteristics. The challenge lies in striking a delicate equilibrium wherein the model remains attuned to authentic seismic events while discarding irrelevant data. Achieving this equilibrium mandates the training of the model on diverse datasets that encapsulate a broad spectrum of noise scenarios and authentic seismic patterns.

Moreover, it is imperative to recognize that the refinement and fine-tuning of the model should remain an ongoing process. This is particularly significant due to the dynamic nature of noise sources, which can evolve over time. As cities expand, infrastructure undertakings progress and the landscape of human activity evolves, the nature of noise embedded within seismic data will inevitably undergo transformations. This dynamic characteristic underscores the necessity for the model to be adaptable rather than static, prepared to accommodate and surmount the challenges that emerge from evolving noise profiles [53].

V. CONCLUSION

This manuscript introduces SeismoNet, an innovative EEW model that capitalizes on a 7-second, three-component seismic waveform record sourced from the CENC. The architecture of the model is characterized by the inclusion of three concurrent dilated convolution layers, which play a pivotal role in the extraction of feature vectors. These vectors are subsequently amalgamated to facilitate the classification process. In response to the challenges stemming from data imbalances within the realm of EEW models, an RL-based

algorithm has been seamlessly integrated. This algorithm rewards the model agent more prominently for precise sample classifications, thereby enhancing its learning process.

The training mechanism of the model is visualized as a sequence of interconnected decision points, with each individual sample treated as a discrete state. Within this framework, the neural network assumes the role of an agent, and its performance in distinguishing between the minority and majority classes is met with corresponding rewards or penalties.

For the initial weight pre-training of the model, a groundbreaking ML-ABC technique is introduced. This method exhibits dynamic adjustments to the optimal "food source" for candidate solutions, ingeniously incorporating mutual learning components that are intricately linked to the initial weights. This innovative initialization process lends the model adaptability and enhances its capacity to learn and adapt during subsequent training phases.

A comprehensive suite of experiments has been conducted using the designated dataset to discern optimal parameter values, including the formulation of the reward function. The outcomes of these experiments resoundingly underscore the efficacy of our proposed methodology when juxtaposed with alternative approaches that were explored within the confines of this study. This affirmation further solidifies the viability and potential of the proposed model as a robust solution for Earthquake Early Warning systems.

ACKNOWLEDGMENT

This study is sponsored by the Key projects of natural science research in Anhui Colleges and Universities: “Research on seismic behavior of vertical irregular steel frame structures based on new composite dampers” (2022AH052653)

This research is sponsored by horizontal topics at the school level: "Research on Energy Dissipation and Damping Technology of Building Structures"(CZZY-HX-2023-08)

REFERENCES

[1] M. R. Jenkins, S. K. McBride, M. Morgoch, and H. Smith, "Considerations for creating equitable and inclusive communication campaigns associated with ShakeAlert, the earthquake early warning system for the West Coast of the USA," Disaster Prevention and Management: An International Journal, vol. 31, no. 1, pp. 79-91, 2022.

[2] E. Zuccolo, G. Cremen, and C. Galasso, "Comparing the performance of regional earthquake early warning algorithms in Europe," Frontiers in Earth Science, vol. 9, p. 686272, 2021.

[3] Y. Nakamura, "On the urgent earthquake detection and alarm system (UrEDAS)," in Proc. of the 9th World Conference on Earthquake Engineering, 1988, vol. 7, pp. 673-678.

[4] R. M. Allen and H. Kanamori, "The potential for earthquake early warning in southern California," Science, vol. 300, no. 5620, pp. 786-789, 2003.

[5] H. Kanamori, "Real-time seismology and earthquake damage mitigation," Annu. Rev. Earth Planet. Sci., vol. 33, pp. 195-214, 2005.

[6] A. Zollo et al., "Earthquake early warning system in southern Italy: Methodologies and performance evaluation," Geophysical research letters, vol. 36, no. 5, 2009.

[7] S. V. Moravvej, S. J. Mousavirad, M. H. Moghadam, and M. Saadatmand, "An LSTM-based plagiarism detection via attention mechanism and a population-based approach for pre-training parameters with imbalanced classes," in Neural Information Processing: 28th International Conference, ICONIP 2021, Sanur, Bali, Indonesia, December 8–12, 2021, Proceedings, Part III 28, 2021: Springer, pp. 690-701.

[8] M. Soleimani, Z. Forouzanfar, M. Soltani, and M. J. Harandi, "Imbalanced Multiclass Medical Data Classification based on Learning Automata and Neural Network," EAI Endorsed Transactions on AI and Robotics, vol. 2, 2023.

[9] G. Haixiang, L. Yijing, J. Shang, G. Mingyun, H. Yuanyue, and G. Bing, "Learning from class-imbalanced data: Review of methods and applications," Expert systems with applications, vol. 73, pp. 220-239, 2017.

[10] S. Moravvej, M. Maleki Kahaki, M. Salimi Sartakhti, and M. Joodaki, "Efficient GAN-based method for extractive summarization," Journal of Electrical and Computer Engineering Innovations (JECEI), vol. 10, no. 2, pp. 287-298, 2022.

[11] S. V. Moravvej, S. J. Mousavirad, D. Oliva, and F. Mohammadi, "A Novel Plagiarism Detection Approach Combining BERT-based Word Embedding, Attention-based LSTMs and an Improved Differential Evolution Algorithm," arXiv preprint arXiv:2305.02374, 2023.

[12] M. S. Sartakhti, M. J. M. Kahaki, S. V. Moravvej, M. javadi Joortani, and A. Bagheri, "Persian language model based on BiLSTM model on COVID-19 corpus," in 2021 5th International Conference on Pattern Recognition and Image Analysis (IPRIA), 2021: IEEE, pp. 1-5.

[13] L. Hong et al., "GAN-LSTM-3D: An efficient method for lung tumour 3D reconstruction enhanced by attention-based LSTM," CAAI Transactions on Intelligence Technology, 2023.

[14] S. V. Moravvej, M. J. M. Kahaki, M. S. Sartakhti, and A. Mirzaei, "A method based on attention mechanism using bidirectional long-short term memory (BLSTM) for question answering," in 2021 29th Iranian Conference on Electrical Engineering (ICEE), 2021: IEEE, pp. 460-464.

[15] S. V. Moravvej, M. Joodaki, M. J. M. Kahaki, and M. S. Sartakhti, "A method based on an attention mechanism to measure the similarity of two sentences," in 2021 7th International Conference on Web Research (ICWR), 2021: IEEE, pp. 238-242.

[16] S. V. Moravvej, A. Mirzaei, and M. Safayani, "Biomedical text summarization using conditional generative adversarial network (CGAN)," arXiv preprint arXiv:2110.11870, 2021.

[17] M. Marani, M. Soltani, M. Bahadori, M. Soleimani, and A. Moshayedi, "The Role of Biometric in Banking: A Review," EAI Endorsed Transactions on AI and Robotics, vol. 2, no. 1, 2023.

[18] M. Bahadori, M. Soltani, M. Soleimani, and M. Bahadori, "Statistical Modeling in Healthcare: Shaping the Future of Medical Research and Healthcare Delivery," in AI and IoT-Based Technologies for Precision Medicine: IGI Global, 2023, pp. 431-446.

[19] S. Vakilian, S. V. Moravvej, and A. Fanian, "Using the cuckoo algorithm to optimizing the response time and energy consumption cost of fog nodes by considering collaboration in the fog layer," in 2021 5th International Conference on Internet of Things and Applications (IoT), 2021: IEEE, pp. 1-5.

[20] D. Karaboga and B. Basturk, "On the performance of artificial bee colony (ABC) algorithm," Applied soft computing, vol. 8, no. 1, pp. 687-697, 2008.

[21] S. V. Moravvej, S. J. Mousavirad, D. Oliva, G. Schaefer, and Z. Sobhaninia, "An improved de algorithm to optimise the learning process of a bert-based plagiarism detection model," in 2022 IEEE Congress on Evolutionary Computation (CEC), 2022: IEEE, pp. 1-7.

[22] S. Vakilian, S. V. Moravvej, and A. Fanian, "Using the artificial bee colony (ABC) algorithm in collaboration with the fog nodes in the Internet of Things three-layer architecture," in 2021 29th Iranian Conference on Electrical Engineering (ICEE), 2021: IEEE, pp. 509-513.

[23] P. Saeid, M. Pazoki, and M. Zeinolabedini, "Optimization of biomass production from sugar bagasse in anaerobic digestion using genetic algorithm," Modeling Earth Systems and Environment, vol. 9, no. 2, pp. 2183-2198, 2023.

[24] S. V. Moravvej et al., "RLMD-PA: A reinforcement learning-based myocarditis diagnosis combined with a population-based algorithm for

pretraining weights," Contrast Media & Molecular Imaging, vol. 2022, 2022.

[25] T. Ren et al., "Seismic severity estimation using convolutional neural network for earthquake early warning," Geophysical Journal International, vol. 234, no. 2, pp. 1355-1362, 2023.

[26] C. Y. Wang, T. C. Huang, and Y. M. Wu, "Using LSTM neural networks for onsite earthquake early warning," Seismological Society of America, vol. 93, no. 2A, pp. 814-826, 2022.

[27] A. Hu and H. Zhang, "Application of machine learning to magnitude estimation in earthquake emergency prediction system," Chinese Journal of Geophysics, vol. 63, no. 7, pp. 2617-2626, 2020.

[28] Y. Wang, Q. Zhao, K. Qian, Z. Wang, Z. Cao, and J. Wang, "Cumulative absolute velocity prediction for earthquake early warning with deep learning," Computer-Aided Civil and Infrastructure Engineering, 2023.

[29] A. Datta, D. J. Wu, W. Zhu, M. Cai, and W. L. Ellsworth, "DeepShake: Shaking intensity prediction using deep spatiotemporal RNNs for earthquake early warning," Seismological Society of America, vol. 93, no. 3, pp. 1636-1649, 2022.

[30] C. Kavitha and V. Gnanadesigan, "Predicting Earthquake Measurements using Deep Learning," in 2023 Eighth International Conference on Science Technology Engineering and Mathematics (ICONSTEM), 2023: IEEE, pp. 1-7.

[31] Y. Wang, X. Li, Z. Wang, and J. Liu, "Deep learning for magnitude prediction in earthquake early warning," Gondwana Research, 2022.

[32] F. Meng, T. Ren, Z. Liu, and Z. Zhong, "Toward earthquake early warning: A convolutional neural network for repaid earthquake magnitude estimation," Artificial Intelligence in Geosciences, vol. 4, pp. 39-46, 2023.

[33] B. Lin et al., "The research of earthquake magnitude determination based on Convolutional Neural Networks," Chinese Journal of Geophysics, vol. 64, no. 10, pp. 3600-3611, 2021.

[34] J. Münchmeyer, D. Bindi, U. Leser, and F. Tilmann, "Earthquake magnitude and location estimation from real time seismic waveforms with a transformer network," Geophysical Journal International, vol. 226, no. 2, pp. 1086-1104, 2021.

[35] H. Zareiamand, A. Darroudi, I. Mohammadi, S. V. Moravvej, S. Danaei, and R. Alizadehsani, "Cardiac Magnetic Resonance Imaging (CMRI) Applications in Patients with Chest Pain in the Emergency Department: A Narrative Review," Diagnostics, vol. 13, no. 16, p. 2667, 2023.

[36] S. Danaei et al., "Myocarditis Diagnosis: A Method using Mutual Learning-Based ABC and Reinforcement Learning," in 2022 IEEE 22nd International Symposium on Computational Intelligence and Informatics and 8th IEEE International Conference on Recent Achievements in Mechatronics, Automation, Computer Science and Robotics (CINTI-MACRo), 2022: IEEE, pp. 000265-000270.

[37] V. François-Lavet, P. Henderson, R. Islam, M. G. Bellemare, and J. Pineau, "An introduction to deep reinforcement learning," Foundations and Trends® in Machine Learning, vol. 11, no. 3-4, pp. 219-354, 2018.

[38] E. Barron and H. Ishii, "The Bellman equation for minimizing the maximum cost," NONLINEAR ANAL. THEORY METHODS APPLIC., vol. 13, no. 9, pp. 1067-1090, 1989.

[39] J. Zhu, S. Li, and J. Song, "Magnitude estimation for earthquake early warning with multiple parameter inputs and a support vector machine," Seismological Research Letters, vol. 93, no. 1, pp. 126-136, 2022.

[40] M. A. Meier et al., "Reliable real-time seismic signal/noise discrimination with machine learning," Journal of Geophysical Research: Solid Earth, vol. 124, no. 1, pp. 788-800, 2019.

[41] J. Huang, X. Wang, Y. Zhao, C. Xin, and H. Xiang, "LARGE EARTHQUAKE MAGNITUDE PREDICTION IN TAIWAN BASED ON DEEP LEARNING NEURAL NETWORK," Neural Network World, no. 2, 2018.

[42] H. Gharagozlou, J. Mohammadzadeh, A. Bastanfard, and S. S. Ghidary, "RLAS-BIABC: A reinforcement learning-based answer selection using the bert model boosted by an improved ABC algorithm," Computational Intelligence and Neuroscience, vol. 2022, 2022.

[43] Ö. Özdemir and E. B. Sönmez, "Weighted cross-entropy for unbalanced data with application on covid x-ray images," in 2020 Innovations in Intelligent Systems and Applications Conference (ASYU), 2020: IEEE, pp. 1-6.

[44] F. Huang, J. Li, and X. Zhu, "Balanced Symmetric Cross Entropy for Large Scale Imbalanced and Noisy Data," arXiv preprint arXiv:2007.01618, 2020.

[45] X. Li, X. Sun, Y. Meng, J. Liang, F. Wu, and J. Li, "Dice loss for data-imbalanced NLP tasks," arXiv preprint arXiv:1911.02855, 2019.

[46] S. S. M. Salehi, D. Erdogmus, and A. Gholipour, "Tversky loss function for image segmentation using 3D fully convolutional deep networks," in Machine Learning in Medical Imaging: 8th International Workshop, MLMI 2017, Held in Conjunction with MICCAI 2017, Quebec City, QC, Canada, September 10, 2017, Proceedings 8, 2017: Springer, pp. 379-387.

[47] S. A. Taghanaki et al., "Combo loss: Handling input and output imbalance in multi-organ segmentation," Computerized Medical Imaging and Graphics, vol. 75, pp. 24-33, 2019.

[48] N. A. Pambudi, "Geothermal power generation in Indonesia, a country within the ring of fire: Current status, future development and policy," Renewable and Sustainable Energy Reviews, vol. 81, pp. 2893-2901, 2018.

[49] A. Shrestha and A. Mahmood, "Review of deep learning algorithms and architectures," IEEE access, vol. 7, pp. 53040-53065, 2019.

[50] Y. Qiu, C. Xu, Z. Xiao, and J. Wang, "Seismogenic Structure of the 2017 M s 6.6 Jinghe, China, Earthquake Inferred from Seismic Detection and Relocation," Seismological Society of America, vol. 93, no. 5, pp. 2612-2624, 2022.

[51] T. Jordan et al., "Operational Earthquake Forecasting: State of Knowledge and Guidelines for Implementation," Annals of Geophysics, 2011.

[52] G. C. Beroza, M. Segou, and S. Mostafa Mousavi, "Machine learning and earthquake forecasting—next steps," Nature communications, vol. 12, no. 1, p. 4761, 2021.

[53] W. Marzocchi and J. D. Zechar, "Earthquake forecasting and earthquake prediction: different approaches for obtaining the best model," Seismological Research Letters, vol. 82, no. 3, pp. 442-448, 2011.